Accepted Manuscript

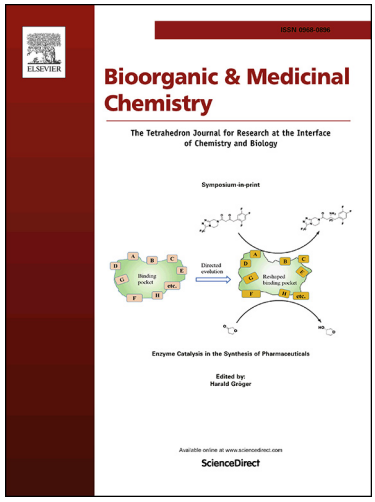

Synthesis and evaluation of novel dimethylpyridazine derivatives as hedgehog signaling pathway inhibitors

Chenglin Wang, Mingfei Zhu, Xiuhong Lu, Hong Wang, Weili Zhao, Xiongwen Zhang, Xiaochun Dong

PII: S0968-0896(18)30492-9
DOI: https://doi.org/10.1016/j.bmc.2018.04.058
Reference: BMC 14341

To appear in: *Bioorganic & Medicinal Chemistry*

Received Date: 9 March 2018
Revised Date: 23 April 2018
Accepted Date: 30 April 2018

Please cite this article as: Wang, C., Zhu, M., Lu, X., Wang, H., Zhao, W., Zhang, X., Dong, X., Synthesis and evaluation of novel dimethylpyridazine derivatives as hedgehog signaling pathway inhibitors, *Bioorganic & Medicinal Chemistry* (2018), doi: https://doi.org/10.1016/j.bmc.2018.04.058

Synthesis and evaluation of novel dimethylpyridazine derivatives as hedgehog signaling pathway inhibitors

Chenglin Wang[a,§], Mingfei Zhu[b,§], Xiuhong Lu[a], Hong Wang[b], Weili Zhao[a], Xiongwen Zhang[b,*], Xiaochun Dong[a,*]

[a]Department of Medicinal Chemistry, School of Pharmacy, Fudan University, Shanghai 201203, P. R. China

[b]Shanghai Engineering Research Center of Molecular Therapeutics and New Drug Development, School of Chemistry and Molecular Engineering, East China Normal University, Shanghai 200062, P. R. China

KEYWORDS: Hedgehog signaling pathway Inhibitors, Anti-tumor agents, dimethylpyridazine,

ABSTRACT:

We report herein the design and synthesis of a series of structural modified dimethylpyridazine compounds as novel hedgehog signaling pathway inhibitors. The bicyclic phthalazine core and 4-methylamino-piperidine moiety of Taladegib were replaced with dimethylpyridazine and different azacycle building blocks, respectively. The in vitro Gli-luciferase assay results demonstrate that the new scaffold still retained potent inhibitory potency. Piperidin-4-amine moiety was found to be the best linker between pharmacophores dimethylpyridazine and fluorine substituted benzoyl group. Furthermore, the optimization of 1-methyl-1H-pyrazol and 4-fluoro-2-(trifluoromethyl)benzamide by different aliphatic or aromatic rings were also investigated and the SAR were described. Several new derivatives were found to show potent Hh signaling inhibitory activity with nanomolar IC_{50} values.

Among these compounds, compound **11c** showed the highest inhibitory potency with an IC_{50} value of 2.33 nM, which was comparable to the lead compound Taladegib. *In vivo* efficacy of **11c** in a $ptch^{+/-}p53^{-/-}$ mouse medulloblastoma allograft model also indicated encouraging results.

AUTHOR INFORMATION

*Corresponding authors. E-mail: xcdong@fudan.edu.cn (X. Dong), xwzhang@sat.ecnu.edu.cn (X. Zhang).

§These authors contributed equally to this paper.

1. Introduction

The hedgehog (Hh) signaling pathway is an evolutionarily conserved signaling axis, which is responsible for patterning and organogenesis in early embryonic development [1]. Under normal conditions, the secreted proteins Sonic hedgehog, Indian hedgehog and Desert hedgehog bind to the negative regulator Patched (Ptch), relieving the suppression of Ptch to a GPCR protein Smoothened (Smo). Smo activation triggers a series of intracellular events ultimately lead to specific gene expression mediated by the Gli family transcription factors [2]. However, mutational activation of Hh has been associated with a variety of cancers, such as basal cell carcinoma (BCC), medulloblastoma (MB), lung, colorectal, prostate, pancreatic, breast and some blood cancers [1,3]. Furthermore, the fact that pharmacological inhibition of Hh signaling could impair the growth of imatinib-resistant mouse and human chronic myelogenous leukemia (CML) makes this signaling pathway attractive to researchers because of the frequent drug-resistant in clinical tumor therapy [4]. Therefore, inhibition of the aberrant Hh signaling represents a promising approach for novel anticancer therapy [3].

Since the natural steroidal alkaloid cyclopamine was identified as the first Smo antagonist to block Hh signaling by directly binding to Smo [5], a number of Smo-targeting small molecules have been developed in recent years. Two agents, Vismodegib (GDC-0449, **1**) and Sonidegib (LDE-225, **2**), have been approved by FDA in 2012 and 2015 for treatment of locally advanced basal cell carcinoma (BCC) [6,7]. In addition, several Hh inhibitors are now in different stages of development including LEQ-506 (phase I, **3**) [8], LY-2940680 (Taladegib, phase II, **4**) [9], IPI-926 (Saridegib, phase II), XL-139 (phase II), PF-04449913 (Glasdegib, phase II) [10] and Itraconazole (phase II) [11].

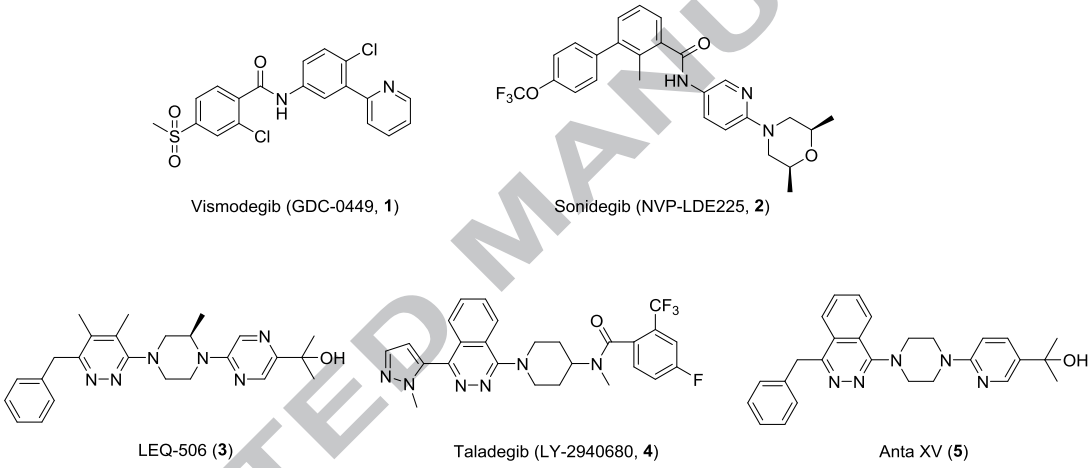

Figure 1. Chemical structure of several Hh signaling pathway inhibitors

During our investigation of novel promising Hh antagonists, we envisioned that the structural modification of Taladegib, which was in an active stage of clinical development, might lead to a new scaffold with better potency and physiochemical properties [9]. The co-crystal structures of the transmembrane domain of the human Smo receptor bound to the Taladegib was reported by Stevens's group in 2013 [12], which have provided a rich set of structural information for drug discovery efforts on Hedgehog pathway inhibitors. Based on the solved co-crystal structure, Taladegib forms three critical hydrogen bonds binding with Smo protein: one hydrogen bond from the amide oxygen atom to N219 residue, two hydrogen bonds between the phthalazine core and R400. Moreover, the

4-fluoro-2-trifluoromethylphenyl moiety of Taladegib forms extensive interactions with residues from ECL3, including Q477, W480, E481 and F484 which stacks to the phenyl ring of Taladegib through π–π interaction. The 4-methylaminopiperidine ring of Taladegib plays an important role as a linker to adjust the orientation of pharmacophores phthalazine and fluorine substituted benzoyl group. [13]

Previously, we have reported our medicinal chemistry efforts on the discovery of novel highly potent Hh inhibitors, which contained a central backbone of phthalazine [14,15]. The piperazine linker of lead compound Anta XV (**5**) was replaced by different four, five and six heterocyclic or spirocyclic building blocks. The most potent compound with piperidin-4-amine moiety was found to possess subnanomolar activity for antagonizing Hh pathway, which was about 12-fold of the potency of Anta XV. This compound also possesses potent antitumor activities both in cell-based assay and *in vivo* allograft studies [14]. Furthermore, we had applied the similar strategy to replace the 4-methylamino-piperidine moiety of Taladegib with different four, five or six-membered azacycle or azaspirocycle building blocks. Several derivatives were found to display potent antitumor activities both in *in vitro* and *in vivo* studies [15].

LEQ-506 (**3**) is another potent second–generation Smo inhibitor discovered by Novartis. The bicyclic phthalazine core of Anta XV (**5**) was replaced with dimethylpyridazine to yield the compound with better potency, decreased hERG activity and improved aqueous solubility [16]. In this study, we choose Taladegib as our lead compound for the development of novel Hh signaling pathway inhibitors. Based on the strategy that Novartis adopted and our early experience in Taladegib modification, we tried to take advantage of the dimethylpyridazine skeleton as a privileged scaffold for phthalazine surrogate and replaced the 4-methylamino-piperidine moiety with different five or six-membered azacycle building blocks to adjust the orientation of pharmacophores dimethylpyridazine and fluorine

substituted benzoyl group (Figure 2, region B). A series of structural modified novel dimethylpyridazine compounds were prepared. Furthermore, the optimization of region A and region C by different aliphatic or aromatic rings were also investigated. Herein, the syntheses and preliminary evaluations *in vitro* are reported.

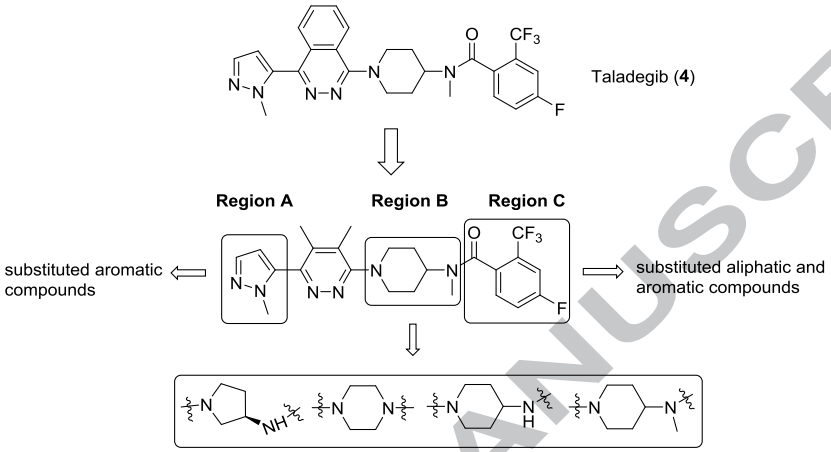

Figure 2: Design concept of novel dimethylpyridazine derivatives.

2. Chemistry

The first round of modification focused on the central linking region B to replace 4-methylamino-piperidine moiety with piperazine, 3-amino-pyrrolidine or 4-amino-piperidine. Four structural modified novel dimethylpyridazine compounds **11a**–**c** and **12** were prepared. As shown in Scheme 1, 3,6-dichloro-4,5-dimethylpyridazine (**7**) was reacted with N-Boc protected five and six-membered azacyclic building blocks **6a**–**c** to give compounds **8a**–**c**. After deprotection with trifluoroacetic acid, the obtained amine **9a**–**c** were then condensed with 4-fluoro-2-(trifluoromethyl)benzoic acid under conventional condensation conditions (HATU, DIPEA, DCM) to give compounds **10a**–**c**. The target molecules **11a**–**c** were finally synthesized through Suzuki coupling using **10a**–**c** reacted with 1-methyl-5-(4,4,5,5-tetramethyl-1,3,2-dioxaborolan-2-yl)-1*H*-pyrazole in the presence of $Pd(PPh_3)_4$ in *m*-xylene assisted by microwave irradiation. Compound **11c** were then methylated with iodomethane to afford the compound **12**.

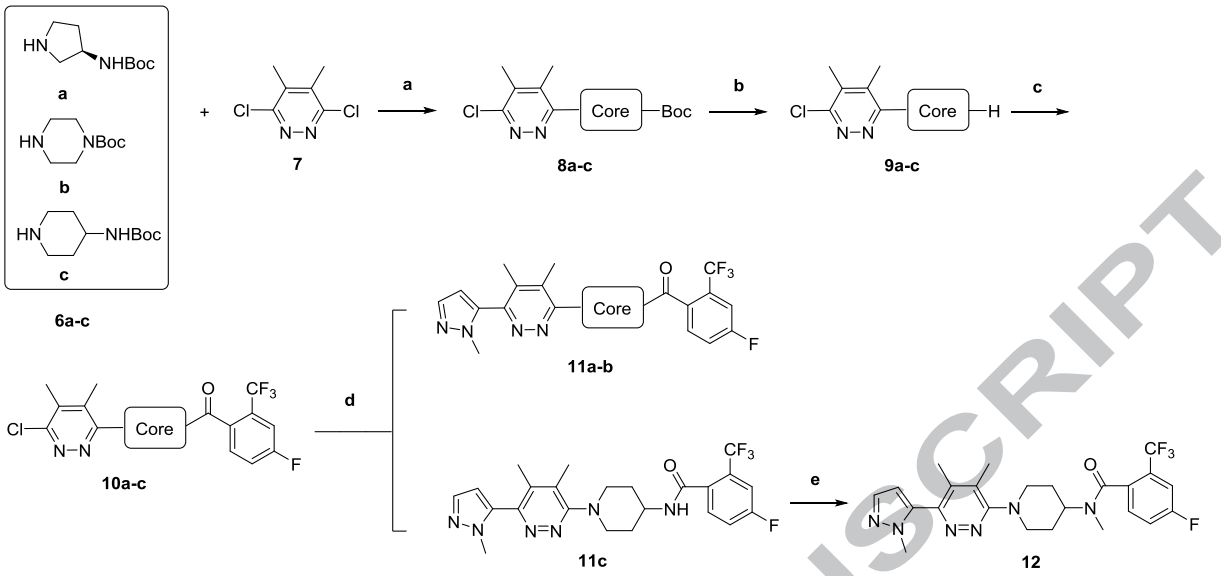

Scheme 1. Synthesis of the compounds **11a-c** and **12**: Reagents and conditions: (a) K_2CO_3, DMF, 110˚C, 7 h, 48–84%; (b) TFA, DCM, rt, 2 h; (c) 4-fluoro-2-(trifluoromethyl)benzoic acid, HATU, DIPEA, DCM, rt, 6 h, 53–76%; (d) 1-methyl-5-(4,4,5,5-tetramethyl-1,3,2-dioxaborolan-2-yl)-1*H*-pyrazole, $Pd(PPh_3)_4$, K_3PO_4, KF, m-xylene, microwave 120 °C, 1 h, 31–35%; (e) CH_3I, NaH, THF, rt, 2 h, 36%.

To our delight, quick assay evaluation (see **Results and discussion**) revealed that dimethylpyridazine derivative with piperidin-4-amine linker (**11c**) led to comparable activity to Taladegib. Thus, the second round of modification fixed the linker region B as piperidin-4-amine and focused on the change in region A. Various aromatic rings were used to replace the 1-methyl-1*H*-pyrazol moiety. The synthesis of designed compounds **13a**–**g** was described in Scheme 2. The above chloride **10c** reacted with different aryl boric acid esters under Suzuki coupling conditions assisted by microwave irradiation in the presence of $Pd(PPh_3)_4$, K_3PO_4 and KF to afford target molecules **13a**–**g**.

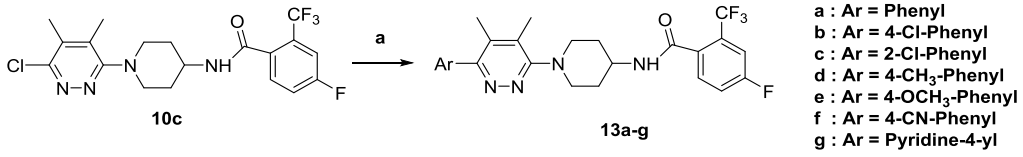

Scheme 2. Synthesis of the compounds **13a-g**: Reagents and conditions: (a) $ArB(OH)_2$, $Pd(PPh_3)_4$, K_3PO_4, KF, *m*-xylene, microwave 120 °C, 1 h, 30–39%.

Unfortunately, the replacement of 1-methyl-1H-pyrazole by different aromatic ring afforded reduced inhibitory effect. Therefore, we retained 1-methyl-1*H*-pyrazole moiety and focused on the change in region C. As depicted in Scheme 3, the N-Boc protected chloride **8c** reacted with 1-methyl-5-(4,4,5,5-tetramethyl-1,3,2-dioxaborolan-2-yl)-1*H*-pyrazole under Suzuki coupling conditions assisted by microwave irradiation to afford compound **14**. After deprotection, intermediate **15** was then reacted with chlorinated aryl esters in NMP at 150 °C with microwave irradiation to afford corresponding esters. Treatment of these esters with CH_3MgI led to the target molecules **16a**–**c**. And target molecule **16d** was obtained by N-arylation of intermediate **15** with 2-bromo-5-(methylsulfonyl)pyrazine in NMP.

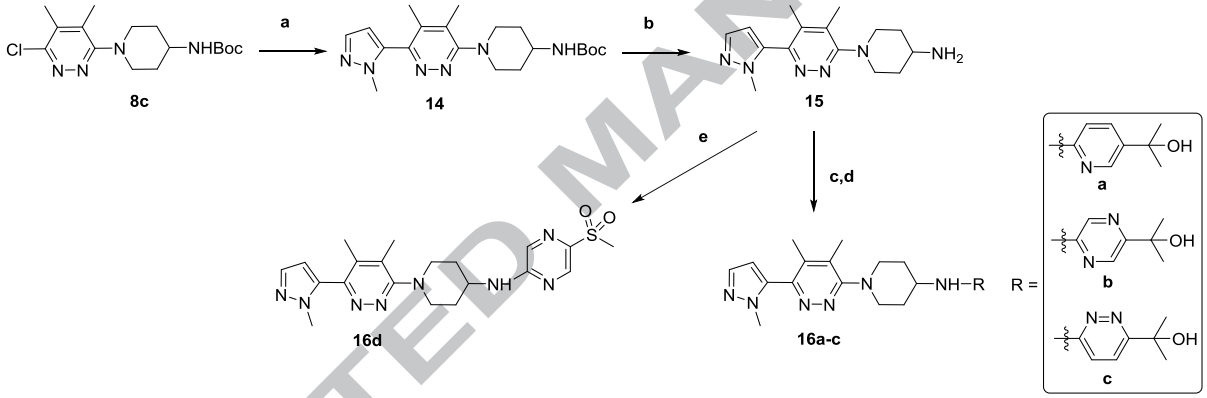

Scheme 3. Synthesis of the compounds **16a**–**d**: Reagents and conditions: (a) 1-methyl-5-(4,4,5,5-tetramethyl-1,3,2-dioxaborolan-2-yl)-1*H*-pyrazole, $Pd(PPh_3)_4$, K_3PO_4, KF, *m*-xylene, microwave 120 °C, 1 h, 53%; (b) TFA, DCM, rt, 2 h; (c) methyl 6-chloronicotinate for **16a** (methyl 5-chloropyrazine-2-carboxylate for 16b, methyl 6-chloropyridazine-3-carboxylate for 16c), Et_3N, NMP, microwave 150 °C, 0.5 h; (d) CH_3MgI, THF, rt, 6 h, 10–22%; (e) 2-bromo-5-(methylsulfonyl) pyrazine, Et_3N, NMP, microwave 150 °C, 0.5 h, 18%.

Meanwhile, we tried to introduce urea, carbamate or amide linkage to connect region B and region C. The synthesis of designed compounds **18a**–**d**, **19**, **20** and **21a**–**e** was described in Scheme 4. Compound **15** was reacted with **17a**–**d** prepared via one step described in Scheme 5 to afford compounds **18a**–**d**. Target molecules **19** was obtained by condensation of **15** with phenyl carbonochloridate in the presence of pyridine. Condensation of **15** with cyclohexyl (4-nitrophenyl) carbonate generated the target compound **20**. Finally, target

compounds **21a**–**e** were prepared by condensation with corresponding benzoic acid under aforementioned standard conditions.

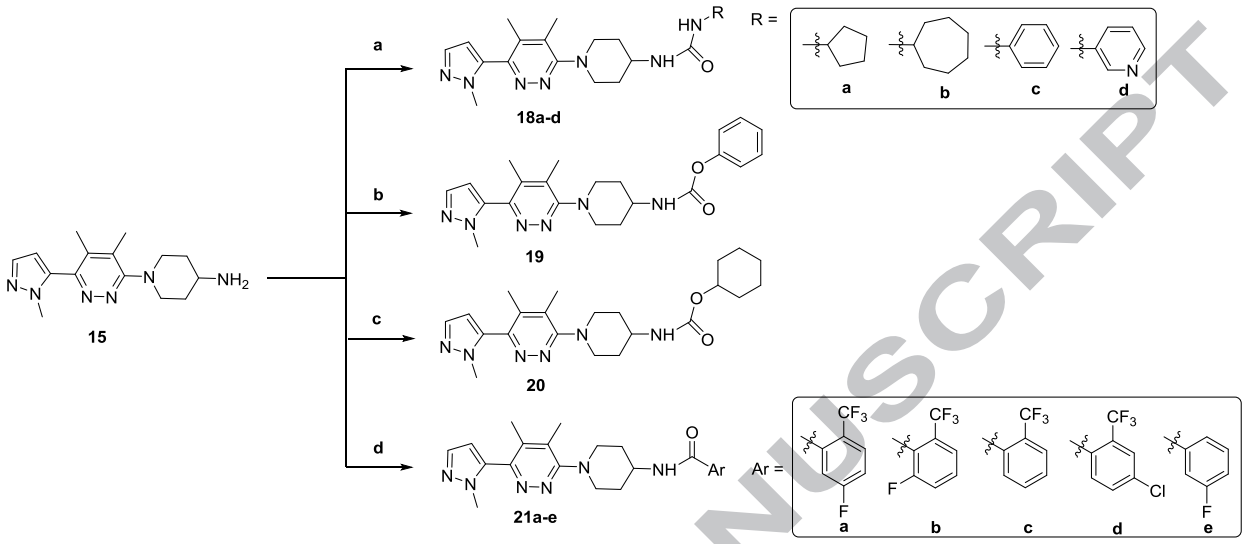

Scheme 4. Synthesis of the compounds **18a**–**d**, **19**, **20** and **21a**–**e**: Reagents and conditions: (a) **17a-d**, Et_3N, DMSO, 100 °C, 8 h, 20-28%; (b) phenyl carbonochloridate, pyridine, DCM, rt, 6 h, 20%; (c) cyclohexyl (4-nitrophenyl) carbonate, DIPEA, THF, rt, 6 h, 16%; (h) corresponding benzoic acid, HATU, DIPEA, DCM, rt, 6 h, 27–43%.

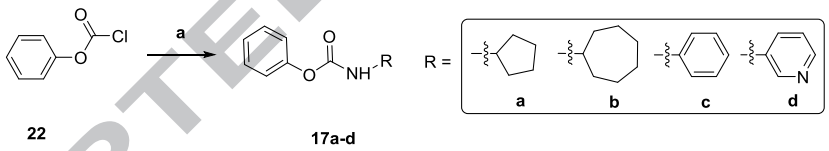

Scheme 5. Synthesis of the compounds **17a**–**d**: Reagents and conditions: (a) corresponding amine, pyridine, DCM, rt, 5 h, 65-80%.

Recently, Xu and collaborators have reported the crystal structure of the multi-domain human Smo, which may inspire the design of a new type of small molecule that links the cysteine-rich domain (CRD) and seven-transmembrane helices domain (TMD), or interacts with the hinge domain (HD) to regulate domain-domain communications that can potentially exert amplified efficacy and overcome drug resistance [17]. Therefore, our next effort was to verify if phenyl-substituted compounds could exhibit moderately enhanced stabilization on Smo [18]. The synthesis of designed compounds **23a**–**c** was described in Scheme 6. These compounds were prepared in 33−40% yields by treating compound **11c** with phenol or

thiophenol under strong basic condition.

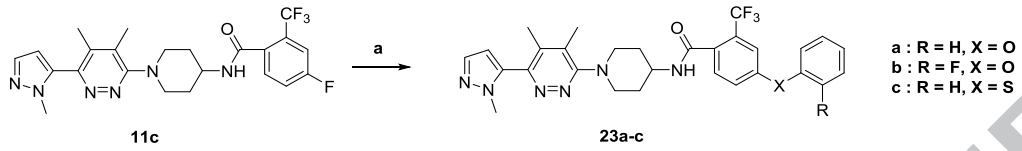

11c 23a-c

Scheme 6. Synthesis of the compounds **24a-c**: Reagents and conditions: (a) phenol or thiophenol, *t*-BuOK, DMSO, 120 °C, 6 h, 33–40%.

3. Results and discussion

3.1. Hh signaling inhibitory activities of the synthesized compounds and the structure-activity relationships (SAR).

All new compounds were evaluated for their ability to inhibit the Hh signaling pathway by dual luciferase reporter assays using light II cells, which were NIH-3T3 cells stably transfected with a Gli-responsive firefly luciferase reporter and Renilla-luciferase expression vector [14,15]. The inhibition rate at 100 nM drug concentration were evaluated first and IC_{50} values were then determined if the inhibition was more than 50%.

The *in vitro* IC_{50} values of compounds **11a**–**c** and **12** were illustrated in Table 1. Both Vismodegib (GDC–0449, **1**) and Taladegib (**4**) were used as positive controls. As expected, replacement of 4-methylamino-piperidine with different five or six-membered heterocyclic building blocks led to significant influences on Hh pathway inhibition. Three of the synthesized compounds exhibit Hedgehog signaling pathway inhibition with IC_{50} values less than 100 nM. To our delight, a change from phthalazine to dimethylpyridazine was well-tolerated (**11c** vs **4**), and the similar inhibition activity was observed (IC_{50} = 2.33 nM). However, N-methylation of compound **11c** resulted in decreased potency (**12** vs **11c**), with IC_{50} value of 29.99 nM. A diminished activity was observed upon replacement of the 4-methylamino-piperidine by pyrrolidin-3-amine (**11a**), with IC_{50} value of 36.39 nM. The

change from 4-methylamino-piperidine to piperazine resulted in the totally loss of activity (**11b**).

Table 1. Inhibition of Compounds to the Hh Pathway Activity Tested by Dual Luciferase Reporter Assays in Light II Cells

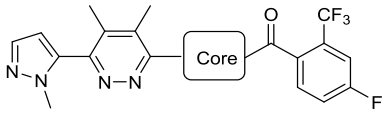

Compounds	core	Inhibition at 100 nM(%)	Gli-luc reporter IC_{50} (nM) [a]
11a	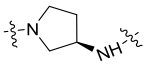	54.13	36.39 ± 5.53
11b	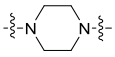	-6.57	>100
11c	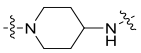	89.49	2.33 ± 0.22
12	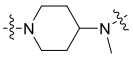	60.87	29.99 ± 4.23
Taladegib (**4**)		94.99	2.26 ± 0.36
Vismodegib (**1**)		108.02	2.46 ± 0.50

[a] Values represent mean ± standard error of three measurements.

Since compound **11c** with dimethylpyridazine moiety was found to possess nanomolar activity in Gli-luciferase reporter assay, which is almost the same as the lead compound Taladegib (**4**). Further optimization of 1-methyl-1*H*-pyrazole component within the dimethylpyridazine derivative **11c** was conducted and the compounds **13a**–**g** were evaluated for their ability to inhibit the Hh signaling pathway. As shown in Table 2, two of the synthesized compounds exhibit inhibitory potency with IC_{50} values less than 10 nM. Replacement of 1-methyl-1*H*-pyrazole by a phenyl ring afforded reduced inhibitory effect (**11c** vs **13a**). Both electron-withdrawing group and electron-releasing group substitutions showed reduced inhibitory effect (compounds **13b**–**f**), compared to compound **11c**. Only the

p-cyano or *o*-chloro substitution show just slightly decreased activity (**11c** vs **13c** and **13f**), with IC_{50} value of 7.02 nM and 8.50 nM, respectively. Meanwhile, replacement of 1-methyl-1*H*-pyrazole by pyridine also diminished the potency, with about 20-fold drop in activity (**11c** vs **13g**).

Table 2. Inhibition of Compounds to the Hh Pathway Activity Tested by Dual Luciferase Reporter Assays in Light II Cells

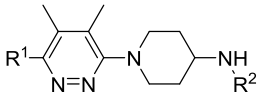

Compounds	R^1	R^2	Inhibition at 100 nM(%)	Gli-luc reporter IC_{50} (nM) [a]
13a		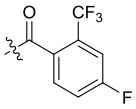	90.17	25.52 ± 4.67
13b	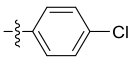	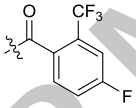	84.99	43.78 ± 1.07
13c		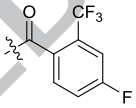	106.32	7.02 ± 0.58
13d		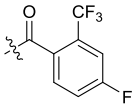	101.41	12.15 ± 7.54
13e	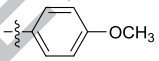	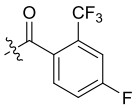	74.52	21.96 ± 2.13
13f	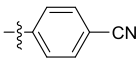	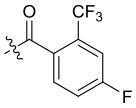	110.94	8.50 ± 1.67
13g		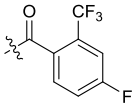	75.97	43.18 ± 8.66
16a		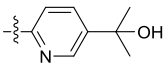	31.84	>100
16b		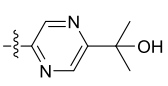	10.82	>100

16c		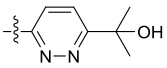	20.61	>100
16d		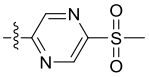	23.80	>100
18a		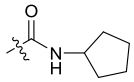	24.35	>100
18b		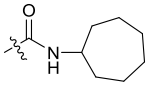	45.73	>100
18c		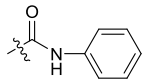	26.23	>100
18d		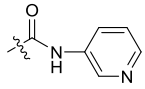	3.47	>100
19		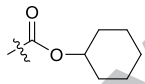	41.19	>100
20		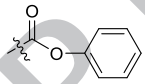	26.65	>100
21a		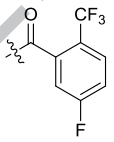	81.96	61.54 ± 7.64
21b		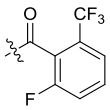	79.80	42.91 ± 4.46
21c		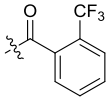	79.66	32.84 ± 2.38
21d		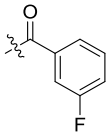	-14.62	>100
21e		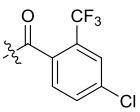	82.11	25.10 ± 3.30

[a] Values represent mean ± standard error of three measurements.

The replacement of 1-methyl-1*H*-pyrazole with different aromatic ring afforded reduced inhibitory effect, thus we retained 1-methyl-1*H*-pyrazole moiety and focused on the change in

region C. Considering that pyridin-3-propanol moiety of ANTA XV (**5**) can form two hydrogen bonds with Smo protein [13], we changed the 4-fluoro-2-trifluoromethylbenzoyl group of compound **13c** with pyridin-3-propanol, pyrazin-2-propanol, pyridazin-3-propanol and 2-methylsulfonylpyrazine to generate four hybrid compounds. Unfortunately, the four new compounds **16a**–**d** showed rather weak inhibitory effects at the concentration of 100 nM Gli-luciferase reporter assay (Table 2). Meanwhile, we used urea and carbamate to connect region B and region C instead of amide. As shown in Table 2, replacement of the amide moiety with urea and carbamate afforded compound **18a**–**d**, **19** and **20** exhibited negligible activity as well. These results may indicate that the huge modification of region C is not tolerated. Therefore, further optimization of region C component within the amide was conducted and the compounds **21a**–**e** were evaluated for their ability to inhibit the Hh signaling pathway. The 5-fluoro-2-(trifluoromethyl)benzamide substituted analog **21a** and 6-fluoro-2-(trifluoromethyl)benzamide substituted analog **21b** showed reduced inhibition against the Hh signaling pathway with an IC_{50} value of 61.54 nM and 42.91 nM, respectively. The replacement of the 4-fluoro-substituent with chlorine resulted in a 10-fold drop in activity (**11c** vs **21e**). The presence of a trifluoromethyl substituent on the aromatic ring, proved to be essential to activity. This strong electron-withdrawing group likely enhanced the π–π interaction with Phe484. Removal of the trifluoromethyl from the 2-position (**21d**) resulted in totally loss of activity, whereas removal of the fluoro from the 4-position (**21c**) led to just 15-fold decrease in inhibition of the Hh pathway.

Introduction of a phenyl ether into Taladegib can strengthen its binding and stabilize the Smo [18], which may inspire the design of new inhibitor that potentially exert amplified efficacy and overcome drug resistance. To further determine the effect of the phenyl-substituted compounds on the Hh pathway activity, compounds **23a**−**c** were designed and tested (Table 3). Gratifyingly, this small series of compounds retained part potency

against the Hh signaling pathway, compounds **23a** and **23b** showing IC_{50} values of 36.47nM and 16.61 nM, respectively. Another thiophenol substituted analogue (**23c**) also retained the potency of 32.46 nM.

Table 3. Inhibition of Compounds to the Hh Pathway Activity Tested by Dual Luciferase Reporter Assays in Light II Cells

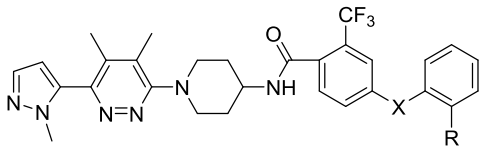

Compounds	X	R	Gli-luc reporter 100 nM(%)	Gli-luc reporter IC_{50} (nM) [a]
23a	O	H	78.90	36.47 ± 5.76
23b	O	F	91.48	16.61 ± 0.99
23c	S	H	82.82	32.46 ± 1.89

[a] Values represent mean ± standard error of three measurements.

*3.2. In vivo efficacy evaluation of compound **11c***

Encouraged by the potent inhibitory activity of compound **11c** on the Gli-luciferase reporter assay, we were eager to know whether the excellent inhibition can be translated into favorable anti-tumor effect. To this end, we focused on the $Ptch^{+/-}p53^{-/-}$ medulloblastoma mouse model, a well-accepted Hh-driven mouse medulloblastoma model that is routinely used to test the efficacy of Hh inhibitors [15]. When the volume of tumors reached around 150–200 mm^3, the tested compound was administered at 10 mg/kg or 20 mg/kg by oral gavage twice a day. As shown in Figure 3, compared to the vehicle control, compound **11c** obviously inhibited the growth of allografted medulloblastoma. And the *in vivo* efficacy of **11c** is slightly more active than the marketed drug Vismodegib (**1**). In addition, **11c** was well tolerated, affording no significant body weight loss at the dose investigated (Figure S1, Supporting Information).

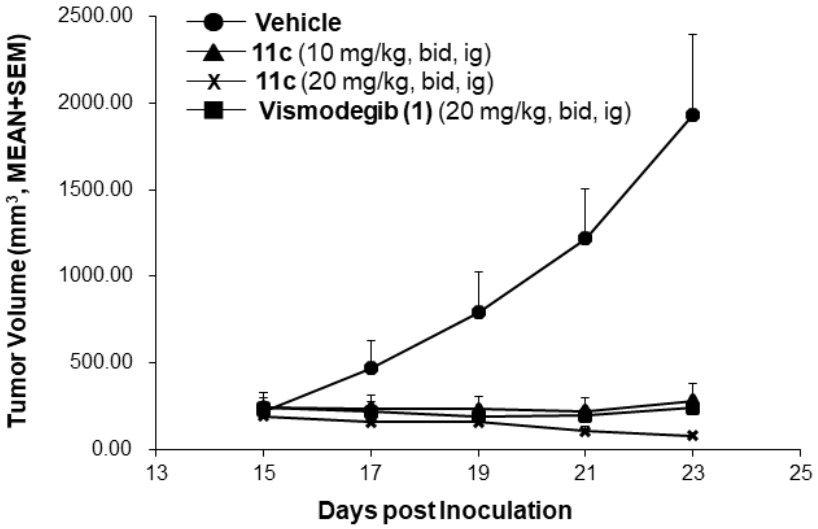

Figure 3. Antitumor activity upon treatment with **11c**, Vismodegib (**1**) or vehicle in $Ptch^{+/-}p53^{-/-}$ medulloblastoma allograft model. Vehicle: 0.5% NaCMC suspension. Tumor volume for indicated days was showed as means ± SEM (n = 5).

3.3. Molecular Docking and Simulation

Molecular docking study was performed to elucidate the binding model of most active compound **11c** into the three-dimensional Smo complex structure (4JKV.pdb) using Schrodinger (Maestro suite). As shown in Figure 4, **11c** forms three critical hydrogen bonds with Smo protein: one hydrogen bond from the amide oxygen atom to Asn219 residue, two hydrogen bonds between the dimethylpyridazine core and Arg400. Furthermore, phenyl ring, pyridazine ring and pyrazol ring interacted with the electron-rich benzene ring of Phe484, Tyr394 and Trp281 via π-π stacking respectively. The docking results demonstrated that the key interactions derived from the Taladegib−Smo crystal complex were almost reserved by our scaffold optimizations. More importantly, **11c** (orange carbons) bind in almost the same location as that of Taladegib (yellow carbons). All these computational predictions suggested that **11c** can exactly interact with ligand binding cavity of Smo and the in silico experiments corroborate well with *in vitro* results.

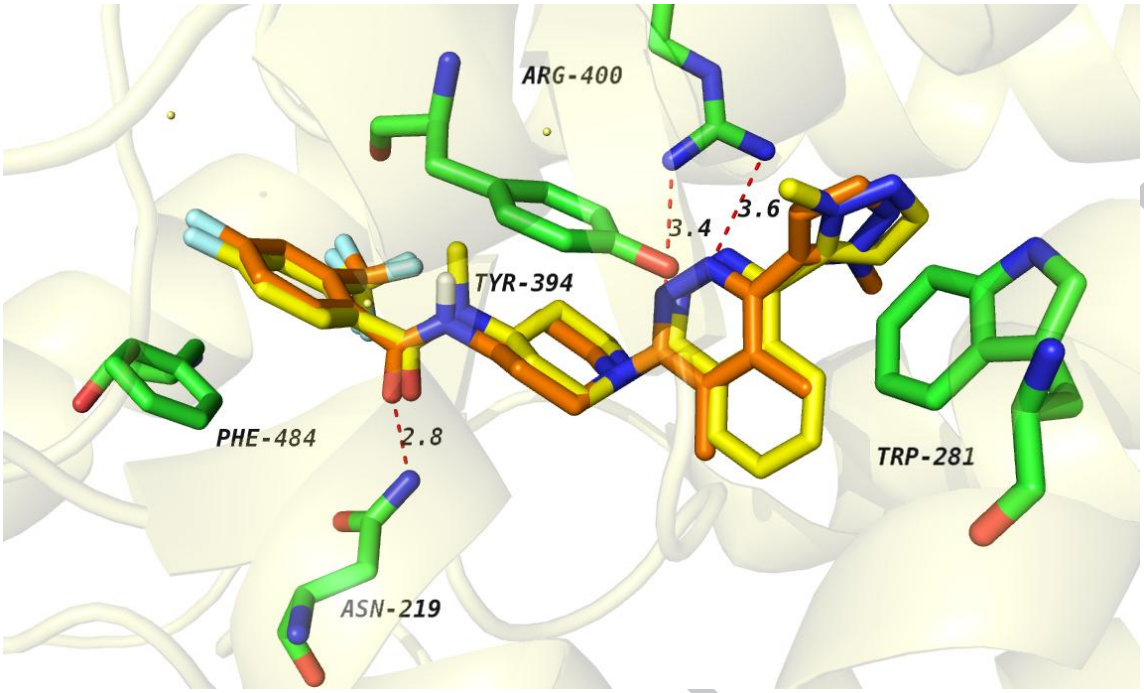

Figure 4. Key interactions of **11c** in the active site of Smo and superposition of **11c** (orange) and Taladegib (yellow). The pictures were generated using Pymol.

4. Conclusion

In summary, a series of structural modified dimethylpyridazine compounds were designed and synthesized. The *in vitro* Gli-luciferase assay results demonstrate that the new scaffold still retained potent inhibitory potency. Piperidin-4-amine moiety was found to be the best linker between pharmacophores dimethylpyridazine and 4-fluoro-2-(trifluoromethyl)benzamide. The expanded comprehensive SAR on region A and C were also investigated and several derivatives were found to show potent Hh signaling inhibitory activity. Among all these compounds, compound **11c** showed the highest inhibitory potency with an IC_{50} value of 2.33 nM, which was comparable to the lead compound Taladegib. Furthermore *in vivo* allograft studies of **11c** also indicated encouraging results.

5. Experimental

5.1. Chemistry

General. All chemicals were purchased from Adamas, SCRC, Alfa Aesar, Acros and used without further purification. Deuterated solvents were purchased from Cambridge Isotope Laboratories. All non-aqueous reactions were carried out using oven-dried (110 °C) or heat gun dried glassware under a positive pressure of dry argon unless otherwise noted. THF and dichloromethane were purified by distillation and dried by passage over activated molecular sieves (type 4 Å) under an argon atmosphere. ^{1}H and ^{13}C NMR data were recorded on a Varian Model Mercury 400 MHz and Bruker 600 MHz spectrometers using solvent signals (DMSO-d_6: δ_H 2.50/δ_C 39.5; $CDCl_3$: δ_H 7.26/δ_C 77.2) as references. ^{1}H NMR chemical shifts (δ) are given in ppm (s = singlet, d = doublet, t = triplet, q = quartet, m = multiplet) downfield from Me_4Si. LC-MS data were recorded on an Agilent 1260/6120 quadrupole LC/MS spectrometer, and High resolution mass spectra obtained on an AB SCIEX Triple TOF^{TM} 5600+ mass spectrometer.

*5.1.1. General procedure for the synthesis of compounds **8a–c***

Solid K_2CO_3 (2 equiv) was added to a solution of 3,6-dichloro-4,5-dimethylpyridazine (1 equiv) and amine (1 equiv) in DMF (20 mL), and the resulting solution was stirred at 110 °C for 7 h. The reaction mixture was concentrated under reduced pressure and dissolved in EtOAc, washed with water, dried over magnesium sulfate, filtered, and concentrated in vacuo. The residue was purified by silica gel column chromatography (ethyl acetate: hexane = 4:1) to yield pure product.

*5.1.1.1. tert-butyl (R)-(1-(6-chloro-4,5-dimethylpyridazin-3-yl)pyrrolidin-3-yl)carbamate (**8a**).* Yellow solid (84%); ^{1}H NMR (400 MHz, $CDCl_3$) δ 4.89 (s, 1H), 4.29 (s, 1H), 3.80–3.61 (m, 2H), 3.57–3.36 (m, 2H), 2.30 (s, 3H), 2.24 (s, 3H), 1.96–1.84 (m, 1H), 1.69 (s, 1H), 1.43 (s, 9H); MS (ESI^+): $[M+H]^+$: 327.2.

*5.1.1.2. tert-butyl 4-(6-chloro-4,5-dimethylpyridazin-3-yl)piperazine-1-carboxylate (**8b**).* White solid (48%); ^{1}H NMR (400 MHz, $CDCl_3$) δ 3.57 (dd, *J* = 6.1, 4.0 Hz, 4H), 3.15 (s, 4H), 2.32 (s, 3H), 2.26 (s, 3H), 1.47 (s, 9H); MS (ESI$^+$): $[M+H]^+$: 327.2.

*5.1.1.3. tert-butyl (1-(6-chloro-4,5-dimethylpyridazin-3-yl)piperidin-4-yl)carbamate (**8c**).* Light yellow solid (80%); ^{1}H NMR (400 MHz, CDCl3) δ 4.55 (s, 1H), 3.69 (s, 1H), 3.43 (d, *J* = 12.9 Hz, 2H), 3.03 (t, *J* = 11.7 Hz, 2H), 2.33 (s, 3H), 2.25 (s, 3H), 2.08 (d, *J* = 10.8 Hz, 2H), 1.59 (d, *J* = 10.8 Hz, 2H), 1.47 (s, 9H); MS (ESI$^+$): $[M+H]^+$: 341.2.

*5.1.2. General procedure for the synthesis of compounds **9a**–**c***

Amide (1 equiv) was dissolved in dichloromethane (20 mL) and charged with TFA (6 equiv) in drops. The mixture was stirred at room temperature for 5 h, and was concentrated afterwards. Without further purification, the crude material was used directly into the next reaction.

*5.1.3. General procedure for the synthesis of compounds **10a**–**c***

DIPEA (0.5 mL) was added to a solution of amine (1 equiv) in dichloromethane (10 mL). The mixture was stirred at 0˚C for 15min. Then 4-fluoro-2-(trifluoromethyl)benzoic acid (1.2 equiv) and HATU (1.2 equiv) were added to the solution, the reaction mixture was stirred for 6 h while warming at room temperature. The reaction solution was washed with water and extracted with dichloromethane, dried over magnesium sulfate, filtered, and concentrated in vacuo. The residue was purified by silica gel column chromatography (dichloromethane: methanol = 30:1) to yield pure product.

5.1.3.1.

*(R)-N-(1-(6-chloro-4,5-dimethylpyridazin-3-yl)pyrrolidin-3-yl)-4-fluoro-2-(trifluoromethyl)benzamide (**10a**).* Yellow solid (76%); ^{1}H NMR (400 MHz, $CDCl_3$) δ 7.51 (dd, *J* = 8.5, 5.4 Hz, 1H), 7.41 (d, *J* = 7.0 Hz, 1H), 7.35 (dd, *J* = 8.8, 2.5 Hz, 1H), 7.16–7.11 (m, 1H), 4.71 (s, 1H),

3.80 (dd, *J* = 11.2, 5.3 Hz, 1H), 3.70 (d, *J* = 11.0 Hz, 1H), 3.65–3.56 (m, 1H), 2.98–2.93 (m, 1H), 2.24 (s, 3H), 2.20 (s, 3H), 2.15 (dd, *J* = 8.0, 4.8 Hz, 2H); MS (ESI^+): $[M+H]^+$: 417.2.

*5.1.3.2. (4-(6-chloro-4,5-dimethylpyridazin-3-yl)piperazin-1-yl)(4-fluoro-2-(trifluoromethyl) phenyl)methanone (**10b**).* White solid (53%); ^1H NMR (400 MHz, $CDCl_3$) δ 7.44 (dd, *J* = 8.7, 2.4 Hz, 1H), 7.38 (dd, *J* = 8.5, 5.4 Hz, 1H), 7.35–7.30 (m, 1H), 4.10–3.97 (m, 1H), 3.91–3.85 (m, 1H), 3.39–3.35 (m, 2H), 3.27–3.17 (m, 4H), 2.34 (s, 3H), 2.28 (s, 3H); MS (ESI^+): $[M+H]^+$: 417.5.

*5.1.3.3. N-(1-(6-chloro-4,5-dimethylpyridazin-3-yl)piperidin-4-yl)-4-fluoro-2-(trifluoromethyl) benzamide (**10c**).* Yellow solid (yield 66%); ^1H NMR (400 MHz, $CDCl_3$) δ 7.58 (dd, *J* = 8.4, 5.5 Hz, 1H), 7.40 (d, *J* = 8.9 Hz, 1H), 7.30 (t, *J* = 8.2 Hz, 1H), 5.84 (d, *J* = 8.0 Hz, 1H), 4.22 (d, *J* = 10.5 Hz, 1H), 3.48 (d, *J* = 13.1 Hz, 2H), 3.11 (t, *J* = 11.9 Hz, 2H), 2.33 (d, *J* = 1.5 Hz, 3H), 2.26 (d, *J* = 2.5 Hz, 3H), 2.18 (d, *J* = 13.0 Hz, 2H), 1.74–1.68 (m, 2H); MS (ESI^+): $[M+H]^+$: 431.2.

*5.1.4. General procedure for the synthesis of compounds **11a**–**c***

Amide pyridazine (1 equiv), borate ester (2 equiv), potassium fluoride (2 equiv), potassium phosphate (2 equiv) and *m*-xylene (5 mL) were added to a microwave vial (20 mL) equipped with a stir bar. The reaction mixture was purged with nitrogen for 2 min. Tetrakis(triphenylphosphine)platinum (0.1 equiv) was added and purged with nitrogen for 2 min again. The vial was sealed and irradiated in the microwave at 120 °C (high absorption setting, Biotage Initiator) for 3 h. The reaction mixture was concentrated under reduced pressure and dissolved in EtOAc (20 mL), washed with water, dried over magnesium sulfate, filtered, and concentrated in vacuo. The residue was purified by silica gel column chromatography (dichloromethane: methanol = 50:1) to yield pure product.

5.1.4.1.

(R)-N-(1-(4,5-dimethyl-6-(1-methyl-1H-pyrazol-5-yl)pyridazin-3-yl)pyrrolidin-3-yl)-4-fluoro-

*2-(trifluoromethyl)benzamide (**11a**).* Yellow solid (31%); ^{1}H NMR (400 MHz, $CDCl_3$) δ 7.58–7.47 (m, 2H), 7.34 (dd, *J* = 8.8, 2.5 Hz, 1H), 7.24 (d, *J* = 7.8 Hz, 1H), 6.61 (d, *J* = 7.0 Hz, 1H), 6.28 (d, *J* = 1.9 Hz, 1H), 4.78–4.66 (m, 1H), 3.87 (dd, *J* = 11.4, 5.6 Hz, 1H), 3.80 (s, 3H), 3.76–3.71 (m, 1H), 3.61–3.53 (m, 1H), 2.25 (s, 3H), 2.16 (s, 3H); ^{13}C NMR (151 MHz, $CDCl_3$) δ 166.70, 160.67, 147.63, 138.47, 138.06, 137.17, 131.95, 131.21 (d, *J* = 8.2), 126.10, 119.05 (d, *J* = 21.2), 114.13, 113.99, 107.68, 55.27, 50.47, 48.59, 37.60, 31.59, 15.92, 15.32. HRMS (ESI) calcd for $C_{22}H_{22}F_4N_6O$ $[M+H]^+$ 463.1864, found 463.1887.

5.1.4.2.

*(4-(4,5-dimethyl-6-(1-methyl-1H-pyrazol-5-yl)pyridazin-3-yl)piperazin-1-yl)(4-fluoro-2-(trifl uoromethyl)phenyl)methanone (**11b**).* Yellow solid (33%); ^{1}H NMR (400 MHz, $CDCl_3$) δ 7.57 (d, *J* = 2.0 Hz, 1H), 7.47–7.30 (m, 3H), 6.37 (d, *J* = 1.9 Hz, 1H), 4.10–4.02 (m, 1H), 3.96 (dd, *J* = 7.3, 3.5 Hz, 1H), 3.92 (s, 3H), 3.39–3.43 (m, 2H), 3.37–3.27 (m, 4H), 2.31 (s, 3H), 2.24 (s, 3H); ^{13}C NMR (151 MHz, $CDCl_3$) δ 166.71, 163.10, 162.14, 161.44, 149.93, 137.97, 130.77, 129.91, 129.70, 129.52 (d, *J* = 8.2), 119.48, 114.49, 108.02, 50.22, 49.44, 47.12, 41.72, 37.90, 16.12, 14.48; HRMS (ESI) calcd for $C_{22}H_{22}F_4N_6O$ $[M+H]^+$ 463.1864, found 463.1867.

5.1.4.3.

*N-(1-(4,5-dimethyl-6-(1-methyl-1H-pyrazol-5-yl)pyridazin-3-yl)piperidin-4-yl)-4-fluoro-2-(tri fluoromethyl)benzamide (**11c**).* White solid (35%); ^{1}H NMR (400 MHz, $CDCl_3$) δ 7.62–7.55 (m, 2H), 7.41 (d, *J* = 8.7 Hz, 1H), 7.31–7.26 (m, 1H), 6.36 (d, *J* = 1.8 Hz, 1H), 5.81 (d, *J* = 7.7 Hz, 1H), 4.28–4.21 (m, 1H), 3.92 (s, 3H), 3.60 (d, *J* = 13.3 Hz, 2H), 3.22–3.15 (m, 2H), 2.29 (s, 3H), 2.22 (s, 3H), 2.20 (s, 2H), 1.80–1.70 (m, 2H); ^{13}C NMR (151 MHz, $CDCl_3$) δ 165.55, 162.17, 148.65, 137.60, 137.36, 136.80, 131.60, 130.54 (d, *J* = 8.3), 129.09, 118.51, 118.37, 113.51, 113.34, 107.26, 48.44, 46.72, 37.22, 31.07, 15.41, 13.97; HRMS (ESI) calcd for $C_{23}H_{24}F_4N_6O$ $[M+H]^+$ 477.2020, found 477.2040.

5.1.5.

*N-(1-(4,5-dimethyl-6-(1-methyl-1H-pyrazol-5-yl)pyridazin-3-yl)piperidin-4-yl)-4-fluoro-N-methyl-2-(trifluoromethyl)benzamide (**12**)*

N-(1-(4,5-dimethyl-6-(1-methyl-1H-pyrazol-5-yl)pyridazin-3-yl)piperidin-4-yl)-4-fluoro-2-(trifluoromethyl)benzamide (**11c**) (100 mg, 0.21 mmol), and NaH (10 mg, 0.42 mmol) were added to THF (20 mL) under nitrogen. The obtained solution was cooled down on an ice-water bath. CH_3I (60 mg, 0.42 mmol) was added to the solution, and the reaction mixture was stirred for 2 h while warming at room temperature. Then the reaction was quenched by addition of saturated NH_4Cl, and the organics were extracted with EtOAc. The organic layers were dried over $MgSO_4$, filtered, and concentrated. The residue was purified by flash chromatography on silica gel (dichloromethane: methanol = 50:1) to yield pure product. Yellow solid (yield 36%). ^{1}H NMR (400 MHz, CDCl3) δ 7.57 (d, *J* = 4.9, 1H), 7.45 (d, *J* = 10.1 Hz, 1H), 7.36–7.33 (m, 2H), 6.36 (d, *J* = 1.8 Hz, 1H), 4.88–4.82 (m, 1H), 3.94 (s, 3H), 3.69 (d, *J* = 13.1 Hz, 2H), 3.29–3.22(m, 2H), 2.73 (s, 3H), 2.30 (s, 3H), 2.23 (s, 3H), 2.22 (s, 2H), 1.93–1.89 (m, 2H). HRMS (ESI) calcd for $C_{24}H_{26}F_4N_6O$ $[M+H]^+$ 491.2177, found 491.2197.

*5.1.6. General procedure for the synthesis of compounds **13a–g***

N-(1-(6-chloro-4,5-dimethylpyridazin-3-yl)piperidin-4-yl)-4-fluoro-2-(trifluoromethyl) benzamide (**10c**) (1 equiv), borate ester (2 equiv), potassium fluoride (2 equiv), potassium phosphate (2 equiv) and *m*-xylene (5 mL) were added to a microwave vial (20 mL) equipped with a stir bar. The reaction mixture was purged with nitrogen for 2 min. Tetrakis(triphenylphosphine)platinum (0.1 equiv) was added and purged with nitrogen for 2 min again. The vial was sealed and irradiated in the microwave at 120 °C (high absorption setting, Biotage Initiator) for 3 h. The reaction mixture was concentrated under reduced pressure and dissolved in EtOAc (20 mL), washed with water, dried over magnesium sulfate,

filtered, and concentrated in vacuo. The residue was purified by silica gel column chromatography (dichloromethane: methanol = 50:1) to yield pure product.

5.1.6.1.

*N-(1-(4,5-dimethyl-6-phenylpyridazin-3-yl)piperidin-4-yl)-4-fluoro-2-(trifluoromethyl) benzamide (**13a**).* Yellow solid (yield 31%); 1H NMR (400 MHz, $CDCl_3$) δ 7.55 (dd, *J* = 8.5, 5.4 Hz, 1H), 7.49–7.45 (m, 3H), 7.43 (d, *J* = 7.9 Hz, 2H), 7.38 (dd, *J* = 9.1, 2.8 Hz, 1H), 7.27 (dd, *J* = 8.8, 3.4 Hz, 1H), 5.95 (d, *J* = 8.0 Hz, 1H), 4.30–4.15 (m, 1H), 3.59–3.48 (m, 2H), 3.22–3.09 (m, 2H), 2.25 (s, 3H), 2.20 (s, 3H), 2.19–2.12 (m, 2H), 1.75–1.71 (m, 2H); ^{13}C NMR (151 MHz, $CDCl_3$) δ 166.16, 162.58, 158.08, 138.04, 135.79, 132.30, 131.23 (d, *J* = 8.2), 129.79, 129.33, 128.20 (d, *J* = 9.1), 119.15, 119.01, 114.12, 113.99, 49.11, 47.40, 31.70, 16.49, 14.44; HRMS (ESI) calcd for $C_{25}H_{24}F_4N_4O$ $[M+H]^+$ 473.1959, found 473.1981.

5.1.6.2.

*N-(1-(6-(4-chlorophenyl)-4,5-dimethylpyridazin-3-yl)piperidin-4-yl)-4-fluoro-2-(trifluoromet hyl)benzamide (**13b**).* Yellow solid (yield 34%); ^1H NMR (400 MHz, $CDCl_3$) δ 7.58 (dd, *J* = 8.5, 5.4 Hz, 1H), 7.44 (d, *J* = 1.1 Hz, 4H), 7.41 (dd, *J* = 8.9, 2.6 Hz, 1H), 7.30 (dd, *J* = 8.1, 2.5 Hz, 1H), 5.90 (d, *J* = 8.1 Hz, 1H), 4.34–4.15 (m, 1H), 3.61–3.52 (m, 2H), 3.21–3.14 (m, 2H), 2.28 (s, 3H), 2.22 (s, 3H), 2.18–2.15 (m, 2H), 1.81–1.71 (m, 2H); ^{13}C NMR (151 MHz, $CDCl_3$) δ 166.15, 162.70, 156.97, 136.49, 135.69, 134.43, 132.27, 131.23 (d, *J* = 8.3), 130.71, 129.88, 128.46, 119.11 (d, *J* = 21.2), 114.16, 49.11, 47.40, 31.70, 29.70, 16.45, 14.49; HRMS (ESI) calcd for $C_{25}H_{23}ClF_4N_4O$ $[M+H]^+$ 507.1569, found 507.1587.

5.1.6.3.

*N-(1-(6-(2-chlorophenyl)-4,5-dimethylpyridazin-3-yl)piperidin-4-yl)-4-fluoro-2-(trifluoromet hyl)benzamide (**13c**).* Yellow solid (yield 33%); ^1H NMR (400 MHz, $CDCl_3$). δ 7.59 (dd, *J* = 8.5, 5.3 Hz, 1H), 7.50–7.45 (m, 1H), 7.43–7.35 (m, 4H), 7.30 (dd, *J* = 8.2, 2.5 Hz, 1H), 5.95 (d, *J* = 8.1 Hz, 1H), 4.32–4.18 (m, 1H), 3.62–3.57 (m, 2H), 3.23–3.16 (m, 2H), 2.28 (s, 3H),

2.20 (d, *J* = 12.8 Hz, 2H), 2.06 (s, 3H), 1.80–1.73(m, 2H); ^{13}C NMR (151 MHz, $CDCl_3$) δ 166.18, 163.09, 156.70, 137.26, 137.07, 135.05, 133.45, 132.30, 131.21 (d, *J* = 8.3), 129.81, 129.38, 129.23, 128.06, 126.95, 119.16, 119.02, 114.18, 49.03, 47.38, 31.74, 31.67, 24.86, 15.72, 14.35; HRMS (ESI) calcd for $C_{25}H_{23}ClF_4N_4O$ $[M+H]^+$ 507.1569, found 507.1580.

5.1.6.4.

*N-(1-(4,5-dimethyl-6-(p-tolyl)pyridazin-3-yl)piperidin-4-yl)-4-fluoro-2-(trifluoromethyl)benz amide (**13d**).* Yellow solid (yield 32%); ^{1}H NMR (400 MHz, $CDCl_3$) δ 7.58 (dd, *J* = 8.5, 5.3 Hz, 1H), 7.44–7.36 (m, 3H), 7.32–7.27 (m, 2H), 7.25 (s, 1H), 5.88 (d, *J* = 8.1 Hz, 1H), 4.33–4.15 (m, 1H), 3.55 (dd, *J* = 11.0, 6.6 Hz, 2H), 3.21–3.14 (m, 2H), 2.42 (s, 3H), 2.27 (s, 3H), 2.23 (s, 3H), 2.21–2.15 (m, 2H), 1.80–1.71 (m, 2H); ^{13}C NMR (151 MHz, $CDCl_3$) δ 166.14, 162.47, 158.11, 138.04, 135.78, 132.31, 131.24 (d, *J* = 8.3), 129.72, 129.25, 128.87, 119.18, 119.04, 114.16, 114.00, 49.12, 47.41, 31.73, 21.30, 16.52, 14.42; HRMS (ESI) calcd for $C_{26}H_{26}F_4N_4O$ $[M+H]^+$ 487.2116, found 487.2138.

5.1.6.5.

*4-fluoro-N-(1-(6-(4-methoxyphenyl)-4,5-dimethylpyridazin-3-yl)piperidin-4-yl)-2-(trifluorom ethyl)benzamide (**13e**).* White solid (yield 35%); ^{1}H NMR (400 MHz, $CDCl_3$) δ 7.55 (dd, *J* = 8.5, 5.4 Hz, 1H), 7.45–7.41 (m, 2H), 7.38 (dd, *J* = 8.9, 2.7 Hz, 1H), 7.24 (dd, *J* = 8.1, 2.5 Hz, 1H), 7.02–6.95 (m, 2H), 6.16 (d, *J* = 8.0 Hz, 1H), 4.34–4.13 (m, 1H), 3.86 (s, 3H), 3.54 (d, *J* = 13.2 Hz, 2H), 3.24–3.08 (m, 2H), 2.26 (s, 3H), 2.23 (s, 3H), 2.17 (dd, *J* = 12.9, 3.6 Hz, 2H), 1.80–1.71 (m, 2H); ^{13}C NMR (151 MHz, $CDCl_3$) δ 166.21, 163.36, 162.40, 161.69, 159.67, 157.71, 135.78, 135.05, 132.34, 131.20 (d, *J* = 8.3), 130.62, 130.52, 130.43, 129.83, 119.06, 118.92, 114.11, 113.95, 113.62, 55.32, 49.14, 47.39, 31.67, 16.55, 14.44; HRMS (ESI) calcd for $C_{26}H_{26}F_4N_4O_2$ $[M+H]^+$ 503.2065, found 503.2079.

5.1.6.6.

N-(1-(6-(4-cyanophenyl)-4,5-dimethylpyridazin-3-yl)piperidin-4-yl)-4-fluoro-2-(trifluorometh

*yl)benzamide (**13f**).* White solid (yield 39%); ^{1}H NMR (400 MHz, $CDCl_3$) δ 7.77 (d, *J* = 8.3 Hz, 2H), 7.67–7.63 (m, 2H), 7.59 (dd, *J* = 8.5, 5.4 Hz, 1H), 7.42 (dd, *J* = 8.8, 2.5 Hz, 1H), 7.33–7.29 (m, 1H), 5.80 (d, *J* = 8.0 Hz, 1H), 4.34–4.17 (m, 1H), 3.60 (d, *J* = 13.3 Hz, 2H), 3.25–3.12 (m, 2H), 2.30 (s, 3H), 2.23 (s, 3H), 2.20 (s, 2H), 1.82–1.69 (m, 2H); ^{13}C NMR (151 MHz, $CDCl_3$) δ 166.15, 162.94, 156.23, 142.64, 135.60, 132.22, 132.06, 131.25 (d, *J* = 8.3), 130.14, 129.97, 119.24, 119.10, 118.66, 114.18, 114.02, 112.17, 49.08, 47.40, 31.69, 16.40, 14.58; HRMS (ESI) calcd for $C_{26}H_{23}F_4N_5O$ $[M+H]^+$ 498.1912, found 498.1931.

5.1.6.7.

*N-(1-(4,5-dimethyl-6-(pyridin-4-yl)pyridazin-3-yl)piperidin-4-yl)-4-fluoro-2-(trifluoromethyl) benzamide (**13g**).* White solid (yield 30%); ^{1}H NMR (400 MHz, $CDCl_3$). δ 8.78–8.67 (m, 2H), 7.59 (dd, *J* = 8.5, 5.3 Hz, 1H), 7.50–7.44 (m, 2H), 7.42 (dd, *J* = 8.8, 2.5 Hz, 1H), 7.31–7.27 (m, 1H), 5.82 (d, *J* = 8.1 Hz, 1H), 4.34–4.16 (m, 1H), 3.61 (d, *J* = 13.2 Hz, 2H), 3.27–3.11 (m, 2H), 2.30 (s, 3H), 2.25 (s, 3H), 2.24–2.17 (m, 2H), 1.77–1.71 (m, 2H); ^{13}C NMR (151 MHz, $CDCl_3$) δ 166.15, 163.05, 155.55, 149.82, 145.77, 135.65, 132.23, 131.28, 131.22, 129.91, 124.06, 119.17 (d, *J* = 21.1), 114.19, 114.02, 49.07, 47.40, 31.69, 16.28, 14.57; HRMS (ESI) calcd for $C_{24}H_{23}F_4N_5O$ $[M+H]^+$ 474.1912, found 474.1931.

5.1.7.

*tert-butyl(1-(4,5-dimethyl-6-(1-methyl-1H-pyrazol-5-yl)pyridazin-3-yl)piperidin-4-yl)carbam ate (**14**).*

The compound was prepared from *tert*-butyl (1-(6-chloro-4,5-dimethylpyridazin-3-yl) piperidin-4-yl)carbamate (**8c**) using the same general procedure that was used for the synthesis of compound **11a**–**c**. Light yellow solid (53%); ^{1}H NMR (400 MHz, $CDCl_3$) δ 7.58 (d, *J* = 1.8 Hz, 1H), 6.37 (d, *J* = 1.7 Hz, 1H), 4.57 (s, 1H), 3.93 (s, 3H), 3.73 (s, 1H), 3.56 (d, *J* = 13.0 Hz, 2H), 3.12 (t, *J* = 11.6 Hz, 2H), 2.28 (s, 3H), 2.23 (s, 3H), 2.11 (d, *J* = 11.9 Hz, 2H), 1.68–1.61 (m, 2H), 1.48 (s, 9H); MS (ESI^+): $[M+H]^+$: 387.5.

5.1.8.

*1-(4,5-dimethyl-6-(1-methyl-1H-pyrazol-5-yl)pyridazin-3-yl)piperidin-4-amine-trifluoroaceta te (**15**).*

The compound was prepared from *tert*-butyl(1-(4,5-dimethyl-6-(1-methyl-1H-pyrazol-5-yl)pyridazin-3-yl)piperidin-4-yl)carbamate (**14**) using the same general procedure that was used for the synthesis of compound **9a**–**c**. Without further purification, the crude material was used directly into the next reaction.

*5.1.9. General procedure for the synthesis of compounds **16a**–**c***

1-(4,5-dimethyl-6-(1-methyl-1H-pyrazol-5-yl)pyridazin-3-yl)piperidin-4-amine-trifluoro acetate (**15**) (1 equiv) and ester (1.5 equiv) were added to a microwave vial (20 ml) equipped with a stir bar. NMP (7 mL) was then added followed by triethylamine (2 ml). The vial was sealed and irradiated in the microwave at 150 °C (high absorption setting) for 30 min. The mixture was then diluted with H_2O and extracted with EtOAc. The organic layers were dried over $MgSO_4$ and concentrated. Without further purification, the crude material was used directly into the next reaction. To a solution of the crude material (1 equiv) in THF (5 mL) at 0 °C was added dropwise CH_3MgI (0.86 mL of 3.0 M solution in Et_2O, 4 equiv). The reaction was stirred for 2 h, and then quenched by addition of saturated NH_4Cl. The mixture was extracted with EtOAc and the organic layer was dried over $MgSO_4$, filtered, concentrated, and then purified by flash chromatography on silica gel (dichloromethane: methanol = 20:1) to afford the title compound **16a**–**c**.

5.1.9.1.

*2-(6-((1-(4,5-dimethyl-6-(1-methyl-1H-pyrazol-5-yl)pyridazin-3-yl)piperidin-4-yl)amino)pyri din-3-yl)propan-2-ol (**16a**).* Light yellow solid (yield 22%); ^{1}H NMR (400 MHz, $CDCl_3$) δ 8.20 (s, 1H), 7.61 (d, *J* = 6.9 Hz, 1H), 7.56 (s, 1H), 6.42 (d, *J* = 8.6 Hz, 1H), 6.36 (s, 1H), 4.64 (s, 1H), 3.92 (s, 4H), 3.60 (d, *J* = 12.0 Hz, 2H), 3.17 (t, *J* = 11.4 Hz, 2H), 2.28 (s, 3H),

2.25 (s, 2H), 2.21 (s, 3H), 1.70 (d, *J* = 10.5 Hz, 2H), 1.56 (s, 6H); ^{13}C NMR (151 MHz, $CDCl_3$) δ 158.62, 157.32, 149.27, 138.30, 138.05, 137.38, 129.72, 124.80, 115.72, 107.90, 71.63, 49.19, 48.49, 37.92, 32.29, 30.39, 16.08, 14.67; HRMS (ESI) calcd for $C_{23}H_{31}N_7O$ $[M+H]^+$ 422.2663, found 422.2678.

5.1.9.2.

*2-(5-((1-(4,5-dimethyl-6-(1-methyl-1H-pyrazol-5-yl)pyridazin-3-yl)piperidin-4-yl)amino)pyrazin-2-yl)propan-2-ol (**16b**).* Light yellow solid (yield 10%); ^{1}H NMR (400 MHz, $CDCl_3$) δ 7.57 (s, 1H), 7.33 (d, *J* = 9.3 Hz, 1H), 6.70 (d, *J* = 9.5 Hz, 1H), 6.36 (s, 1H), 4.68 (s, 1H), 4.17 (s, 1H), 3.93 (s, 3H), 3.63 (d, *J* = 10.8 Hz, 2H), 3.21 (t, *J* = 11.6 Hz, 2H), 2.30 (s, 2H), 2.29 (s, 3H), 2.23 (s, 3H), 1.76 (d, *J* = 10.5 Hz, 2H), 1.56 (s, 6H); ^{13}C NMR (151 MHz, $CDCl_3$) δ 157.38, 149.26, 138.30, 138.05, 137.38, 129.71, 124.70, 115.69, 107.90, 71.62, 49.19, 48.46, 37.91, 32.30, 30.39, 16.08, 14.67; HRMS (ESI) calcd for $C_{22}H_{30}N_8O$ $[M+H]^+$ 423.2615, found 423.2611.

5.1.9.3.

*2-(6-((1-(4,5-dimethyl-6-(1-methyl-1H-pyrazol-5-yl)pyridazin-3-yl)piperidin-4-yl)amino)pyridazin-3-yl)propan-2-ol (**16c**).* Light yellow solid (yield 12%); ^{1}H NMR (400 MHz, $CDCl_3$) δ 7.58 (s, 1H), 7.33 (d, *J* = 8.9 Hz, 1H), 6.70 (d, *J* = 9.3 Hz, 1H), 6.37 (s, 1H), 4.57 (s, 1H), 4.22 (s, 1H), 3.93 (s, 3H), 3.64 (d, *J* = 13.3 Hz, 2H), 3.21 (t, *J* = 11.5 Hz, 2H), 2.33 (S, *2*H), 2.30 (s, 3H), 1.81–1.71 (m, 2H), 1.56 (s, 6H); ^{13}C NMR (151 MHz, $CDCl_3$) δ 162.79, 154.97, 142.42, 140.72, 138.20, 138.10, 137.58, 129.82, 107.95, 48.95, 48.28, 41.44, 37.90, 31.77, 29.69, 16.10, 14.65; HRMS (ESI) calcd for $C_{22}H_{30}N_8O$ $[M+H]^+$ 423.2615, found 423.2613.

5.1.10.

*N-(1-(4,5-dimethyl-6-(1-methyl-1H-pyrazol-5-yl)pyridazin-3-yl)piperidin-4-yl)-5-(methylsulfonyl)pyrazin-2-amine (**16d**).*

1-(4,5-dimethyl-6-(1-methyl-1H-pyrazol-5-yl)pyridazin-3-yl)piperidin-4-amine-trifluoro acetate (**15**) (300 mg, 1.05 mmol) and 2-bromo-5-(methylsulfonyl)pyrazine (360 mg, 1.5 mmol) were added to a microwave vial (20 ml) equipped with a stir bar. NMP (7 mL) was then added followed by triethylamine (2 ml). The vial was sealed and irradiated in the microwave at 150 °C (high absorption setting) for 30 min. The mixture was then diluted with H_2O and extracted with EtOAc. The organic layers were dried over $MgSO_4$, filtered, and concentrated. The residue was purified by flash chromatography on silica gel (dichloromethane: methanol = 10:1) to yield pure product. Light yellow solid (yield 18%); ^{1}H NMR (400 MHz, $CDCl_3$) δ 8.66 (s, 1H), 7.93 (s, 1H), 7.56 (s, 1H), 6.36 (s, 1H), 5.72 (d, *J* = 6.6 Hz, 1H), 4.17 (s, 1H), 3.90 (s, 3H), 3.62 (d, *J* = 12.7 Hz, 2H), 3.20 (t, *J* = 11.4 Hz, 2H), 3.13 (s, 3H), 2.29 (s, 3H), 2.22 (s, 3H), 2.18 (s, 2H), 1.76 (d, *J* = 10.6 Hz, 2H); ^{13}C NMR (151 MHz, $CDCl_3$) δ 152.69, 149.53, 138.59, 138.05, 137.52, 137.00, 129.83, 125.48, 107.72, 71.02, 56.33, 51.26, 48.57, 37.78, 31.93, 30.40, 30.37, 29.70, 29.36, 15.95, 15.47; HRMS (ESI) calcd for $C_{20}H_{26}N_8O_2S$ $[M+H]^+$ 443.1972, found 443.1993.

*5.1.11. General procedure for the synthesis of compounds **17a–d***

Amine (1 equiv) was dissolve in dichloromethane (10 mL). The obtained solution was cooled down on an ice-water bath. Then phenyl carbonochloridate (1.2 equiv), pyridine (1.2 equiv) were added in order. The reaction mixture was stirred for 5 h while warming at room temperature, and was concentrated afterwards. Without further purification, the crude material was used directly into the next reaction.

*5.1.11. General procedure for the synthesis of compounds **18a–d***

1-(4,5-dimethyl-6-(1-methyl-1H-pyrazol-5-yl)pyridazin-3-yl)piperidin-4-amine-trifluoro acetate (**15**) (1.6 equiv), carbamate (1 equiv) and triethylamine (2 equiv) were added to DMSO (5 mL) under nitrogen. The mixture was then stirred at 100 °C for 8 h. The reaction solution was washed with water and extracted with EtOAc, dried over magnesium sulfate,

filtered, and concentrated in vacuo. The residue was purified by silica gel column chromatography (dichloromethane: methanol = 20:1) to yield pure product.

*5.1.11.1. 1-cyclopentyl-3-(1-(4,5-dimethyl-6-(1-methyl-1H-pyrazol-5-yl)pyridazin-3-yl) piperidin-4-yl)urea(**18a**).* White solid (yield 20%); ^{1}H NMR (400 MHz, $CDCl_3$) δ 7.56 (d, *J* = 1.7 Hz, 1H), 6.35 (d, *J* = 1.7 Hz, 1H), 4.63 (s, 2H), 3.96 (dd, *J* = 13.3, 6.5 Hz, 1H), 3.91 (s, 3H), 3.54 (d, *J* = 12.9 Hz, 2H), 3.13 (t, *J* = 11.3 Hz, 2H), 2.27 (s, 3H), 2.21 (s, 3H), 2.09 (d, *J* = 10.7 Hz, 2H), 1.97–1.93 (m, 4H), 1.66–1.56 (m, 4H), 1.39–1.36 (m, 2H); ^{13}C NMR (151 MHz, $CDCl_3$) δ 162.94, 157.18, 149.12, 138.31, 138.04, 137.33, 129.66, 107.89, 52.26, 49.17, 47.11, 37.90, 33.66, 32.91, 23.62, 16.06, 14.68; HRMS (ESI) calcd for $C_{21}H_{31}N_7O$ $[M+H]^+$ 398.2663, found 398.2663.

*5.1.11.2. 1-cycloheptyl-3-(1-(4,5-dimethyl-6-(1-methyl-1H-pyrazol-5-yl)pyridazin-3-yl) piperidin-4-yl)urea (**18b**).* White solid (yield 25%); ^{1}H NMR (400 MHz, $CDCl_3$) δ 7.62 (d, *J* = 1.9 Hz, 1H), 6.42 (s, 1H), 3.90 (s, 3H), 3.82 (s, 1H), 3.65 (d, *J* = 14.1 Hz, 3H), 3.21 (t, *J* = 11.9 Hz, 2H), 2.33 (s, 3H), 2.26 (s, 3H), 2.11 (d, *J* = 12.6 Hz, 2H), 1.95 (d, *J* = 13.8 Hz, 2H), 1.76–1.68 (m, 2H), 1.65–1.59 (m, 4H), 1.54–1.46 (m, 6H). ^{13}C NMR (151 MHz, $CDCl_3$) δ 162.94, 156.57, 149.13, 138.04, 129.65, 107.89, 51.52, 49.18, 47.21, 41.04, 37.90, 35.75, 32.92, 28.11, 24.08, 16.05, 14.67; HRMS (ESI) calcd for $C_{23}H_{35}N_7O$ $[M+H]^+$ 426.2976, found 426.2976.

5.1.11.3.

*1-(1-(4,5-dimethyl-6-(1-methyl-1H-pyrazol-5-yl)pyridazin-3-yl)piperidin-4-yl)-3-phenylurea (**18c**).* Yellow solid (yield 28%); ^{1}H NMR (400 MHz, $CDCl_3$) δ 7.56 (s, 1H), 7.28 (s, 3H), 7.03 (s, 2H), 6.35 (s, 1H), 5.26 (d, *J* = 6.7 Hz, 1H), 3.97 (s, 1H), 3.88 (s, 3H), 3.51 (d, *J* = 13.3 Hz, 2H), 3.13 (t, *J* = 11.6 Hz, 2H), 2.63 (s, 1H), 2.25 (s, 3H), 2.20 (s, 3H), 2.06 (s, 2H), 1.61 (d, *J* = 9.8 Hz, 2H); ^{13}C NMR (151 MHz, $CDCl_3$) δ 155.17, 138.75, 138.19 (d, *J* = 19.6),

137.59, 129.93, 129.25, 123.62, 120.74, 107.94, 48.93, 46.89, 37.84, 32.44, 16.07, 14.75; HRMS (ESI) calcd for $C_{22}H_{27}N_7O$ $[M+H]^+$ 406.2350, found 406.2368.

5.1.11.4.

*1-(1-(4,5-dimethyl-6-(1-methyl-1H-pyrazol-5-yl)pyridazin-3-yl)piperidin-4-yl)-3-(pyridin-3-yl)urea (**18d**).* Yellow solid (yield 22%); ^{1}H NMR (400 MHz, $CDCl_3$) δ 8.55 (s, 1H), 8.44 (s, 1H), 8.26–8.14 (m, 2H), 7.54 (d, *J* = 1.7 Hz, 1H), 6.37 (s, 1H), 6.10 (d, *J* = 6.8 Hz, 1H), 3.98 (s, 1H), 3.86 (s, 3H), 3.45 (s, 2H), 3.13 (dd, *J* = 13.3, 8.6 Hz, 2H), 2.29 (s, 3H), 2.20 (s, 3H), 1.60 (d, *J* = 8.8 Hz, 2H), 1.39 (dd, *J* = 16.2, 8.8 Hz, 2H); ^{13}C NMR (151 MHz, $CDCl_3$) δ 163.41, 154.98, 149.25, 142.61, 139.83, 138.25, 138.10, 137.24, 130.80, 126.80, 124.11, 108.03, 48.39, 46.07, 37.77, 31.83, 16.08, 14.72, 8.68; HRMS (ESI) calcd for $C_{21}H_{26}N_8O$ $[M+H]^+$ 407.2302, found 407.2319.

5.1.12. Phenyl

*(1-(4,5-dimethyl-6-(1-methyl-1H-pyrazol-5-yl)pyridazin-3-yl)piperidin-4-yl)carbamate (**19**).*

1-(4,5-dimethyl-6-(1-methyl-1H-pyrazol-5-yl)pyridazin-3-yl)piperidin-4-amine-trifluoro acetate (**15**) (100 mg, 0.25 mmol) was dissolved in dichloromethane (10 mL) and charged with pyridine (200 mg, 2.5 mmol) in drops. The mixture was stirred at room temperature for 10 min, then phenyl carbonochloridate (46 mg, 0.3 mmol) was added. The obtained solution was stirred at room temperature for 6 h. The mixture was then diluted with H_2O and extracted with methylene chloride. The organic layers were dried over $MgSO_4$ and concentrated. The residue was purified by flash chromatography on silica gel (dichloromethane: methanol = 20:1) to afford the title compound **19**. Yellow solid (yield 20%); ^{1}H NMR (400 MHz, $CDCl_3$) δ 7.57 (s, 1H), 7.36 (t, *J* = 7.7 Hz, 2H), 7.20 (t, *J* = 7.5 Hz, 1H), 7.14 (d, *J* = 7.9 Hz, 2H), 6.36 (s, 1H), 5.08 (d, *J* = 7.8 Hz, 1H), 3.92 (s, 3H), 3.86 (s, 1H), 3.59 (d, *J* = 13.3 Hz, 2H), 3.15 (t, *J* = 11.5 Hz, 2H), 2.28 (s, 3H), 2.22 (s, 3H), 2.18 (s, 2H), 1.75 (dd, *J* = 20.4, 10.5 Hz, 2H); ^{13}C NMR (151 MHz, $CDCl_3$) δ 162.83, 153.75, 149.31, 138.24, 138.04, 137.41, 129.73,

129.31, 125.34, 121.55, 107.93, 49.05, 48.41, 37.92, 32.30, 16.09, 14.63; HRMS (ESI) calcd for $C_{22}H_{26}N_6O_2$ $[M+H]^+$ 407.2190, found 407.2205.

*5.1.13. Cyclohexyl (1-(4,5-dimethyl-6-(1-methyl-1H-pyrazol-5-yl)pyridazin-3-yl)piperidin-4-yl)carbamate (**20**).*

To the solution of cyclohexyl (4-nitrophenyl) carbonate (100 mg, 0.25 mmol) in THF (5 mL) was added DIPEA (200 mg), the mixture was allowed to stir in an ice bath for 10 min. Then compound **15** (132 mg, 0.5 mmol) was added to the solution, and the reaction mixture was stirred for 6 h while warming at room temperature. The reaction solution was washed with water and extracted with EtOAc, dried over magnesium sulfate, filtered, and concentrated in vacuo. The residue was purified by silica gel column chromatography (dichloromethane: methanol = 20:1) to yield pure product. Yellow solid (yield 16%); ^{1}H NMR (400 MHz, $CDCl_3$) δ 6.37–6.36 (m, 1H), 4.66 (d, *J* = 8.0 Hz, 2H), 3.95–3.89 (m, 3H), 3.76 (d, *J* = 10.2 Hz, 1H), 3.56 (d, *J* = 12.6 Hz, 2H), 3.15–3.09 (m, 2H), 2.28 (d, *J* = 2.6 Hz, 3H), 2.22 (d, *J* = 2.6 Hz, 3H), 2.13 (d, *J* = 12.4 Hz, 2H), 1.89 (s, 2H), 1.77–1.69 (m, 2H), 1.65 (d, *J* = 11.0 Hz, 2H), 1.54 (s, 2H), 1.40–1.36 (m, 4H). ^{13}C NMR (151 MHz, $CDCl_3$) δ 162.91, 155.48, 138.26, 138.03, 137.38, 132.09 (d, *J* = 10.4), 129.75, 128.55 (d, *J* = 12.1), 107.92, 49.10, 37.90, 32.50, 32.06, 25.42, 23.85, 16.07, 14.63; HRMS (ESI) calcd for $C_{22}H_{32}N_6O_2$ $[M+H]^+$ 413.2660, found 413.2673.

*5.1.14. General procedure for the synthesis of compounds **21a**–**e***

The compound was prepared from 1-(4,5-dimethyl-6-(1-methyl-1H-pyrazol-5-yl) pyridazin-3-yl)piperidin-4-amine-trifluoroacetate (**15**) using the same general procedure that was used for the synthesis of compound **10a**–**c**.

*5.1.14.1. N-(1-(4,5-dimethyl-6-(1-methyl-1H-pyrazol-5-yl)pyridazin-3-yl)piperidin-4-yl)-5-fluoro-2-(trifluoromethyl)benzamide (**21a**).* White solid (yield 31%); ^{1}H NMR (400 MHz, $CDCl_3$) δ 7.72

(dd, *J* = 8.8, 5.0 Hz, 1H), 7.57 (d, *J* = 1.8 Hz, 1H), 7.30–7.27 (m, 1H), 7.25–7.20 (m, 1H), 6.36 (d, *J* = 1.9 Hz, 1H), 5.91 (d, *J* = 8.0 Hz, 1H), 4.26 (d, *J* = 10.4 Hz, 1H), 3.92 (s, 3H), 3.62 (d, *J* = 13.1 Hz, 2H), 3.24–3.18 (m, 2H), 2.30 (s, 3H), 2.23 (s, 3H), 2.20 (s, 2H), 1.81–1.72 (m, 2H); ^{13}C NMR (151 MHz, $CDCl_3$) δ 165.00, 161.98, 148.54, 137.95, 137.40, 137.18, 129.43, 128.41, 116.24 (d, *J* = 21.6), 115.72 (d, *J* = 23.8), 107.37, 48.42, 46.69, 37.28, 31.03, 15.49, 14.10; HRMS (ESI) calcd for $C_{23}H_{24}F_4N_6O$ $[M+H]^+$ 477.2020, found 477.2044.

5.1.14.2.

*N-(1-(4,5-dimethyl-6-(1-methyl-1H-pyrazol-5-yl)pyridazin-3-yl)piperidin-4-yl)-2-fluoro-6-(trifluoromethyl)benzamide (**21b**).* White solid (yield 27%); ^{1}H NMR (400 MHz, $CDCl_3$) δ 7.57 (d, *J* = 1.7 Hz, 1H), 7.53–7.50 (m, 2H), 7.39–7.30 (m, 1H), 6.37 (d, *J* = 1.9 Hz, 1H), 5.93 (d, *J* = 8.0 Hz, 1H), 4.31 (dd, *J* = 12.7, 7.1 Hz, 1H), 3.92 (s, 3H), 3.62 (d, *J* = 13.0 Hz, 2H), 3.25–3.19 (m, 2H), 2.30 (s, 3H), 2.26 (s, 2H), 2.23 (s, 3H), 1.78 (m, 2H); ^{13}C NMR (151 MHz, $CDCl_3$) δ 161.95, 161.09, 148.47, 137.39, 137.31, 137.24, 130.50 (d, *J* = 8.4), 129.51, 121.42, 119.25, 119.10, 107.39, 48.40, 46.59, 37.31, 31.01, 15.52, 14.14; HRMS (ESI) calcd for $C_{23}H_{24}F_4N_6O$ $[M+H]^+$ 477.2020, found 477.2022.

5.1.14.3.

*N-(1-(4,5-dimethyl-6-(1-methyl-1H-pyrazol-5-yl)pyridazin-3-yl)piperidin-4-yl)-2-(trifluoromethyl)benzamide (**21c**).* White solid (yield 43%); ^{1}H NMR (400 MHz,$CDCl_3$) δ 7.72 (d, *J* = 7.6 Hz, 1H), 7.65–7.54 (m, 4H), 6.36 (d, *J* = 1.9 Hz, 1H), 5.80 (d, *J* = 8.0 Hz, 1H), 4.35–4.21 (m, 1H), 3.92 (s, 3H), 3.60 (d, *J* = 13.2 Hz, 2H), 3.27–3.14 (m, 2H), 2.29 (s, 3H), 2.25 (s, 2H), 2.23 (s, 3H), 1.81–1.69 (m, 2H); ^{13}C NMR (151 MHz, $CDCl_3$) δ 166.53, 137.61, 137.40, 136.77, 135.33, 131.49, 129.22, 129.06, 128.07, 125.70, 107.27, 48.44, 46.58, 37.27, 31.16, 15.43, 13.99; HRMS (ESI) calcd for $C_{23}H_{25}F_3N_6O$ $[M+H]^+$ 459.2115, found 459.2118.

5.1.14.4.

4-chloro-N-(1-(4,5-dimethyl-6-(1-methyl-1H-pyrazol-5-yl)pyridazin-3-yl)piperidin-4-yl)-2-(tr

*ifluoromethyl)benzamide (**21d**).* White solid (yield 27%); ^{1}H NMR (400 MHz, $CDCl_3$) δ 7.69 (s, 1H), 7.62–7.48 (m, 3H), 6.36 (d, *J* = 2.1 Hz, 1H), 5.81 (d, *J* = 8.0 Hz, 1H), 4.25 (d, *J* = 10.5 Hz, 1H), 3.91 (d, *J* = 2.1 Hz, 3H), 3.60 (d, *J* = 13.2 Hz, 2H), 3.22–3.16 (m, 2H), 2.29 (s, 3H), 2.22 (s, 3H), 2.20 (s, 2H), 1.80–1.70 (m, 2H); ^{13}C NMR (151 MHz, $CDCl_3$) δ 166.09, 162.80, 138.23, 138.04, 137.44, 136.13, 134.31, 132.25, 130.31, 129.72, 126.69, 107.92, 49.06, 47.39, 37.91, 31.74, 16.08, 14.62; HRMS (ESI) calcd for $C_{23}H_{24}ClF_3N_6O$ $[M+H]^+$ 493.1725, found 493.1746.

5.1.14.5.

*N-(1-(4,5-dimethyl-6-(1-methyl-1H-pyrazol-5-yl)pyridazin-3-yl)piperidin-4-yl)-3-fluorobenza mide (**21e**).* White solid (yield 34%); ^{1}H NMR (400 MHz, $CDCl_3$) δ 7.80 (dd, *J* = 8.7, 5.4 Hz, 2H), 7.58 (d, *J* = 1.9 Hz, 1H), 7.15–7.11 (m, 2H), 6.37 (d, *J* = 1.9 Hz, 1H), 6.06 (d, *J* = 7.8 Hz, 1H), 4.32–4.20 (m, 1H), 3.93 (s, 3H), 3.62 (d, *J* = 13.2 Hz, 2H), 3.28–3.14 (m, 2H), 2.30 (s, 3H), 2.23 (s, 3H), 2.20 (s, 2H),1.83–1.73 (m, *J* = 11.1, 3.7 Hz, 2H); ^{13}C NMR (151 MHz, $CDCl_3$) δ 165.81, 162.85, 149.33, 138.25, 138.06, 137.42, 130.82, 129.70, 129.17 (d, *J* = 9.0), 115.73, 115.59, 107.92, 49.14, 47.04, 37.91, 32.16, 16.08, 14.64; HRMS (ESI) calcd for $C_{22}H_{25}FN_6O$ $[M+H]^+$ 409.2147, found 409.2165.

*5.1.15. General procedure for the synthesis of compounds **23a**–**c***

N-(1-(4,5-dimethyl-6-(1-methyl-1H-pyrazol-5-yl)pyridazin-3-yl)piperidin-4-yl)-4-fluoro -2-(trifluoromethyl)benzamide (**11c**) (1 equiv), phenol or thiophenol (2 equiv) and *t*-BuOK (2 equiv) were added to DMSO (5 mL) under nitrogen. The mixture was then stirred at 120 °C for 6 h. The reaction solution was washed with water and extracted with dichloromethane, dried over magnesium sulfate, filtered, and concentrated in vacuo. The residue was purified by silica gel column chromatography (dichloromethane: methanol = 40:1) to yield pure product.

5.1.15.1.

*N-(1-(4,5-dimethyl-6-(1-methyl-1H-pyrazol-5-yl)pyridazin-3-yl)piperidin-4-yl)-4-phenoxy-2-(trifluoromethyl)benzamide (**23a**).* Yellow solid (yield 40%); ^{1}H NMR (400 MHz, $CDCl_3$) δ 7.59–7.49 (m, 2H), 7.42–7.38 (m, 2H), 7.29 (d, *J* = 2.3 Hz, 1H), 7.23–7.19 (m, 1H), 7.13 (dd, *J* = 8.4, 2.3 Hz, 1H), 7.03 (d, *J* = 8.0 Hz, 2H), 6.35 (d, *J* = 1.9 Hz, 1H), 4.25 (d, *J* = 10.5 Hz, 1H), 3.90 (s, 3H), 3.59 (d, *J* = 13.1 Hz, 2H), 3.15–3.21 (m, 2H), 2.28 (s, 3H), 2.21 (s, 3H), 2.19 (s, 2H), 1.74–1.67 (m, 2H); ^{13}C NMR (151 MHz, $CDCl_3$) δ 158.19, 154.76, 137.61, 137.40, 136.83, 130.10, 129.55 (d, *J* = 14.2), 129.13, 124.19, 120.21, 119.13, 115.38, 115.34, 107.29, 48.43, 46.61, 37.26, 31.13, 29.07, 15.45, 14.02; HRMS (ESI) calcd for $C_{29}H_{29}F_3N_6O_2$ $[M+H]^+$ 551.2377, found 551.2377.

5.1.15.2.

*N-(1-(4,5-dimethyl-6-(1-methyl-1H-pyrazol-5-yl)pyridazin-3-yl)piperidin-4-yl)-4-(2-fluorophenoxy)-2-(trifluoromethyl)benzamide (**23b**).* White solid (yield 33%); ^{1}H NMR (400 MHz, $CDCl_3$) δ 7.62–7.45 (m, 2H), 7.27 (s, 1H), 7.23 (d, *J* = 4.4 Hz, 1H), 7.21 (s, 1H), 7.19–7.16 (m, 1H), 7.14 (d, *J* = 7.3 Hz, 1H), 7.08 (dd, *J* = 8.6, 2.3 Hz, 1H), 6.35 (d, *J* = 1.8 Hz, 1H), 4.25–4.20 (m, 1H), 3.90 (d, *J* = 1.3 Hz, 3H), 3.59 (d, *J* = 13.1 Hz, 2H), 3.21–3.15 (m, 2H), 2.28 (s, 3H), 2.23 (s, 2H), 2.21 (s, 3H) 1.79–1.73 (m, 2H); ^{13}C NMR (151 MHz, $CDCl_3$) δ 166.10, 162.20, 157.96, 148.65, 137.61, 137.40, 136.81, 130.11, 129.64, 129.12, 125.90, 124.59, 122.20, 118.64, 116.96, 116.84, 114.01, 107.28, 48.44, 46.63, 37.26, 31.13, 29.06, 27.78, 15.44, 14.01; HRMS (ESI) calcd for $C_{29}H_{28}F_4N_6O_2$ $[M+H]^+$ 569.2283, found 569.2299.

5.1.15.3.

*N-(1-(4,5-dimethyl-6-(1-methyl-1H-pyrazol-5-yl)pyridazin-3-yl)piperidin-4-yl)-4-(phenylthio)-2-(trifluoromethyl)benzamide (**23c**).* White solid (yield 35%); ^{1}H NMR (400 MHz, $CDCl_3$) δ 7.57–7.56 (m, 1H), 7.53 (d, *J* = 1.8 Hz, 1H), 7.46 (dd, *J* = 7.5, 2.8 Hz, 2H), 7.44–7.38 (m,

4H), 7.35 (d, *J* = 8.0 Hz, 1H), 6.36 (dd, *J* = 2.0, 1.2 Hz, 1H), 5.76 (d, *J* = 8.0 Hz, 1H), 4.26–4.19 (m, 1H), 3.92 (d, *J* = 1.3 Hz, 3H), 3.59 (d, *J* = 13.2 Hz, 2H), 3.22–3.16 (m, 2H), 2.28 (s, 3H), 2.22 (s, 3H), 2.19 (s, 2H), 1.79–1.66 (m, 2H); ^{13}C NMR (151 MHz, $CDCl_3$) δ 166.71, 162.80, 149.30, 141.31, 138.22, 138.04, 137.44, 133.42, 131.65, 129.79 (d, *J* = 14.2), 128.93, 126.00, 107.93, 49.04, 47.23, 37.92, 31.75, 16.09, 14.65; HRMS (ESI) calcd for $C_{29}H_{29}F_3N_6OS$ $[M+H]^+$ 567.2148, found 567.2151.

5.2. Biological assay

5.2.1. In vitro Dual-luciferase reporter assay to evaluate the Hh signaling pathway inhibitory activity

Light II cells were kindly provided by Professor. Philip Beachy from Stanford University and maintained in DMEM containing 10% fetal bovine serum (FBS), zeocin 0.15 mg/mL and G418 0.4 mg/mL at 37°C in a 5% CO_2 atmosphere. Cells seeded in 96-well plates were treated with various compounds for 48h as indicated. The luciferase activity in the cell lysates was examined with a Dual-Luciferase Reporter Assay System (Promega) according to the manufacturer's instructions in a luminometer (Molecular Devices; Sunnyvale, CA). The firefly luciferase values were normalized to *Renilla* values.

5.2.2. In vivo anti-tumor effects in medulloblastoma allograft model

$Ptch^{+/-}p53^{-/-}$ mice were obtained by crossing $ptch^{+/-}$ mice (Jackson Laboratory; Bar Harbor, ME) with $p53^{-/-}$ mice (Jackson Laboratory). The primary intracranial medulloblastomas spontaneously aroused in $Ptch^{+/-}p53^{-/-}$ mice were harvested and subcutaneously allografted into athymic nude mice (Beijing HFK Bio-Technology; Beijing, China). After well-developed, the tumors were collected, cut into 1 mm^3 fragments, and inoculated subcutaneously into the right flank of athymic nude mice using a trocar. When the tumor volume reached 150–200 mm^3, the mice were administered with vehicle or tested

compound by oral gavage twice a day. The tumor growth was recorded with the measurement of length (L) and width (W) by caliper every other day and calculated as tumor volume (V) = $L \times W^2/2$. Meanwhile, the body weights of mice were recorded. Five animals were used for all groups and tumor volume for indicated days was showed as means ± SEM.

Acknowledgments

This work was supported by NSFC (21572037).

References

1. Pomeroy SL, Tamayo P, Gaasenbeek M, et al. *Nature*. 2002;415:436-442.
2. (a) Varjosalo M, Taipale J. *Genes Dev*. 2008;22:2454-2472. (b) Jiang J, Hui CC. *Dev. Cell*.2008;15:801-812.
3. Rubin LL, de Sauvage FJ. *Nat Rev Drug Discov*. 2006;5:1026-1033.
4. Zhao C, Chen A, Jamieson CH, et al. *Nature*. 2009;458:776-779.
5. Cooper MK, Porter JA, Young KE, Beachy PA. *Science*. 1998;280:1603-1607.
6. Robarge KD, Brunton SA, Castanedo GM, et al. *Bioorg Med Chem Lett*. 2009;19:5576-5581.
7. Pan S, Wu X, Jiang J, et al. *ACS Med Chem Lett.* 2010;1:130-134.
8. Peukert S, He F, Dai M, et al. *ChemMedChem*. 2013;8:1261-1265
9. Bender MH, Hipskind PA, Capen AR, et al. *Cancer Res*. 2011;71:2819.
10. (a)Tremblay MR, Nesler M, Weatherhead R, Castro AC. *Expert Opin Ther Pat.* 2009;19:1039-1056.(b) Hadden MK. *Expert Opin Ther Pat*. 2013;23:345-361. (c) Xin, M. *Expert Opin Ther Pat.*,2015;25:549-565.
11. Gan GN, Jimeno A. *Expert Opin Investig Drugs*. 2016;25:1153-1166.

12. Wang C, Wu H, Katritch V, et al. *Nature*. 2013;497:338-3343.

13. Wang C, Wu H, Evron T, et al. *Nat Commun*. 2014;5:4355.

14. Bao X, Peng Y, Lu X, et al. *Bioorg Med Chem Lett*. 2016;26:3048-3051.

15. Lu X, Peng Y, Wang C, et al. *Eur J Med Chem*. 2017;138:384-395.

16. Peukert S, He F, Dai M, et al. *ChemMedChem*. 2013;8:1261-1265.

17. Zhang X, Zhao F, Wu Y, et al. *Nat Commun*. 2017;8:15383.

18. Ye L, Ding K, Zhao F, et al. *Med. Chem. Commun.* 2017;8:1332-1336.

Graphical abstract ：

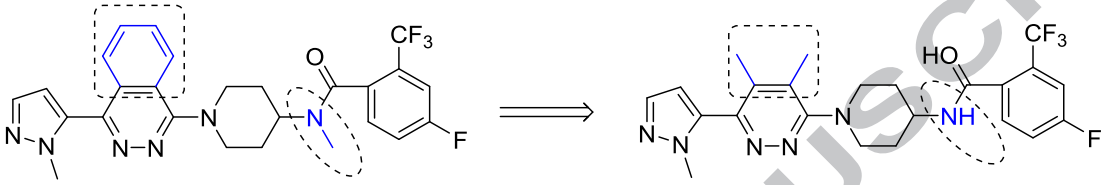

Taladegib

IC_{50}=2.26nM

11c

IC_{50}=2.33nM